

Spaced-Antenna Aperture Synthesis Using an X-Band Active Phased-Array

V. Venkatesh[✉], K. Orzel[✉], and S. Frasier[✉]

Abstract—Spaced antenna (SA) radars retrieve wind-fields by tracking resolution volume sized bins of scatterers as they advect between two physically displaced antennas. To date, SA methods have been applied for profiling the ionosphere and precipitation free atmosphere. The primary technological difficulty in applying these methods to probe precipitation at microwave frequencies is the requirement for such a short antenna separation that a significant overlap in apertures is necessary. In this article, we synthesize overlapped apertures by segmenting active phased-arrays into subarrays that are multiplexed in time. Antenna pattern measurements are then employed to evaluate beamforming errors on a family of implementations. Based on measurements and Monte Carlo simulations, we find that highly overlapping apertures are most immune to beam squint errors. This is because element-level phase errors are retained on the synthesized SAs and differential beam squint errors are minimized. Finally, we demonstrate a novel method to measure relative phase center displacement between SAs that obviates the need for near-field antenna measurements.

Index Terms—Phased array, spaced antenna (SA), X-band radar.

I. INTRODUCTION

SPACED antenna (SA) radars correlate received signals from two displaced apertures to retrieve the wind field component along the baseline. These SA radars have been routinely employed for measuring baseline wind components in the ionosphere and atmospheric boundary layer [1], [2]. The low radar frequencies in these applications allowed for baselines that were relatively large in comparison to the antenna dimension. This is because the correlation time of the backscattered signal is inversely proportional to radar frequency. Long correlation times in turn allowed for long baselines.

The “see-saw” relationship between radar frequency and baseline makes the design parameters for SA weather radars at microwave frequencies challenging. SA weather radars must have a short baseline and significantly overlapping apertures to sample the spatial fading pattern before significant

Manuscript received November 9, 2019; revised January 21, 2020; accepted February 23, 2020. Date of publication May 28, 2020; date of current version June 24, 2021. This work was supported by the National Science Foundation under Grant AGS-0937768 and Grant AGS-1318148. (*Corresponding author:* V. Venkatesh.)

V. Venkatesh is with the Jet Propulsion Laboratory, California Institute of Technology, Pasadena, CA 91125 USA, and also with the Department of Electrical and Computer Engineering, University of Massachusetts Amherst, Amherst, MA 01003 USA (e-mail: vijay.venkatesh@jpl.nasa.gov).

K. Orzel and S. Frasier are with the Department of Electrical and Computer Engineering, University of Massachusetts Amherst, Amherst, MA 01003 USA.

Digital Object Identifier 10.1109/LGRS.2020.2995360

decorrelation occurs. If methods to synthesize closely spaced apertures with sufficient isolation are developed, the SA method may potentially allow significant improvements in the spatial resolution of wind field retrievals. This is because existing methods in the community such as velocity-azimuth-display (VAD) rely on the scanning capability of weather radars to retrieve the large-scale wind field over a 360° azimuthal swath, whereas the SA method measures the local wind field within a single resolution cell.

Previous schemes to implement overlapping apertures for SA weather radars employed polarization diversity to isolate antennas [3] and a passive phased-array antenna system in a monopulse configuration [4]. The first approach relied on separable yet well-correlated scattering of orthogonal polarizations by hydrometeors. For this dual-polarized SA (DPSA) system design, a low duty cycle transmitter restricted the pulse repetition frequency to be too small to adequately sample the correlation function. But more importantly, the mechanical motion of the beam complicated retrieval of cross-beam wind fields.

The National Weather Radar Testbed (NWRT) overcame difficulties due to mechanical scanning by employing a passive phased-array aperture. For the spaced-antenna implementation on the NWRT [4], equally dividing the array face into left and right receive subarrays resulted in a baseline that was so long that hydrometeor reshuffling in the resolution volume degraded retrieval precision. Although this was an important step toward realizing SA weather radars, the fixed monopulse configuration provided little means to further optimize for spaced-antenna retrievals.

To date, literature on applying the spaced-antenna method to precipitation has focused on improving models of the correlation function to account for the independent motion of hydrometeors in the resolution volume [4] and idealized retrieval studies based on simulations [5]. This article focuses on SA weather radar aperture synthesis using an X-band active phased array. Active phased arrays offer flexibility in aperture synthesis but are sensitive to errors in beamforming. Section II outlines the design specifics of the active phased-array spaced-antenna system. Based on measurements and simulations, Section III then evaluates errors in RF beamforming on differently sized spaced-antenna sub-arrays.

II. ACTIVE PHASED-ARRAY SPACED-ANTENNA CONCEPT

The X-band “phase-tilt” radar system was developed by a team of engineers from the Microwave Remote Sensing Lab (MIRSL) at the University of Massachusetts [6] and

1545-598X © 2020 IEEE. Personal use is permitted, but republication/redistribution requires IEEE permission.
See <https://www.ieee.org/publications/rights/index.html> for more information.

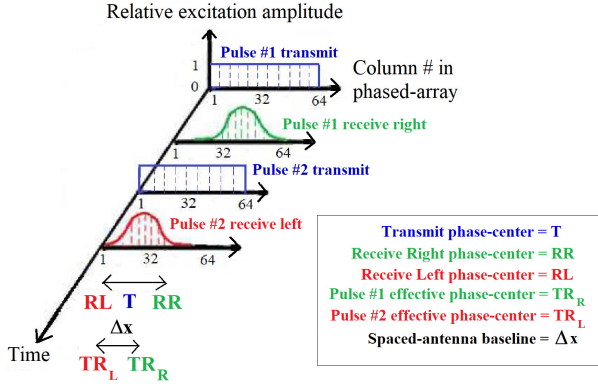


Fig. 1. Time series of transmit/receive aperture weighting indicating left and right receive apertures interleaved with the transmit aperture. The effective SA baseline is denoted by Δx .

the center for collaborative and adaptive sensing of the atmosphere (CASA) [7]. This system comprises a linear array antenna, programmable transmit/receive modules, a master field-programmable gate array (FPGA) controller and a host computer. The antenna array has a peak transmit power of 64 W and consists of 64 “stick” element. Each “stick” is a series-fed microstrip patch array with a peak transmit power of 1 W. The full array has a 1.6° beamwidth in the azimuth plane and a 3.5° beamwidth in the elevation plane at broadside. Behind each antenna element, a transmit/receive (T/R) module provides independent amplitude and phase control. The T/R modules are synchronized by clocking signals provided by the master FPGA controller. A beam scheduling module on the host computer preload beam sequences that are executed by the state machines residing in the FPGA.

Fig. 1 depicts the approach to implementing a spaced-antenna system on an active phased-array radar. The entire array can be used upon transmit in order to maximize elemental contributions to transmit power. Alternating subarrays with displaced phase-centers are used on receive. The effective phase centers of the overlapped apertures are located midway between the centers of the transmit and receive apertures. Auto- and cross correlation functions may be produced with interleaved time series from separate portions of the array and enable retrievals of baseline wind. Many spaced-antenna system designs were implemented on the active phased-array radar system. The first family of implementations was an electronically scanned 2.6° spaced-antenna system. Here, a 2.1° aperture was employed on transmit aperture and a 4° aperture was employed on receive. Since both the aperture dimension and the aperture separation follow a cosine roll-off across electronic scan angle, they are compensated in order to provide near-constant values across scan-angle. This allowed fixed cross correlation statistics as a function of scan angle and simplified interpretation. The second family of spaced-antenna systems focused on broadside implementations and allowed further evaluation of RF beamforming errors.

In the following section, the implemented spaced-antenna designs are evaluated in terms of three figures of merit: differences between measured and desired beamwidths, differences between measured and desired baselines,

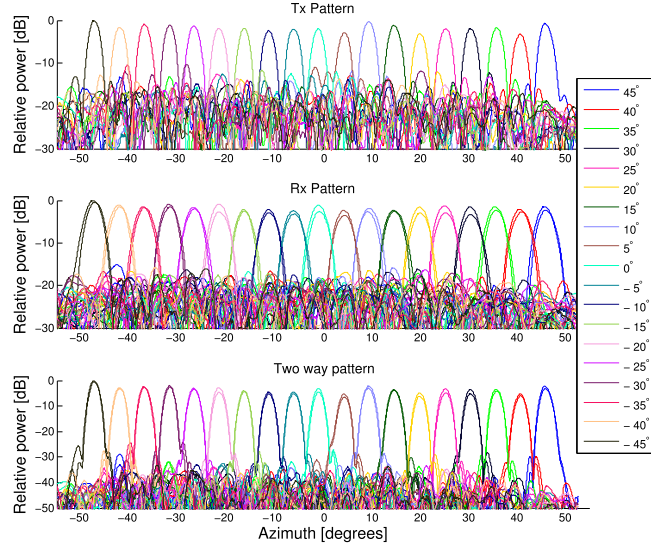


Fig. 2. Azimuthal scans of a beacon using the 2.6° equivalent one-way beamwidth spaced-antenna system. The patterns were measured by mechanically slewing the array face past a beacon.

and relative beam squint between the equivalent monostatic left and right apertures. These performance metrics are primarily synthesized from far-field pattern measurements. Where necessary, “simulated” values are used as a prognostic. These simulated values take T/R module failure into account, and add pseudorandom numbers to the desired weighting to mimic quantization errors. Rayleigh statistics for rms amplitude errors and uniform distributions for rms phase errors were assumed [8]. Beamwidths were then calculated from the corresponding far-field patterns assuming no mutual coupling between the elements. Furthermore, the simple simulation methodology employed herein does not incorporate element level differences in subarrays such as mutual coupling and edge effects. Lastly, a novel method is demonstrated to gauge the implemented baseline.

III. APERTURE SYNTHESIS RESULTS

A. Beamwidth Measurements

Fig. 2 shows qualitative results of antenna far-field measurements for the electronically scanned 2.6° spaced-antenna systems. Beam locations spanning -45° to 45° in steps of 5° were implemented. The first subplot shows far-field patterns corresponding to the transmit beam. The second panel shows receive antenna patterns with the left and right subarrays overlaid for each beam location. Unlike the transmit pattern where a uniform aperture weighting resulted in sidelobes of approximately 13 dB, the receive pattern corresponds to a Taylor weighting applied across the subarray and has significantly lower sidelobes. The bottom panel shows two-way patterns that are obtained by multiplying the transmit and receive patterns. As expected, the two-way pattern corresponding to the left and right spaced-antenna apertures are similar.

Some comments about the far-field pattern measurement methodology in Fig. 2 are in order. A pyramidal horn located at a distance of 85 m from the array was used as a source

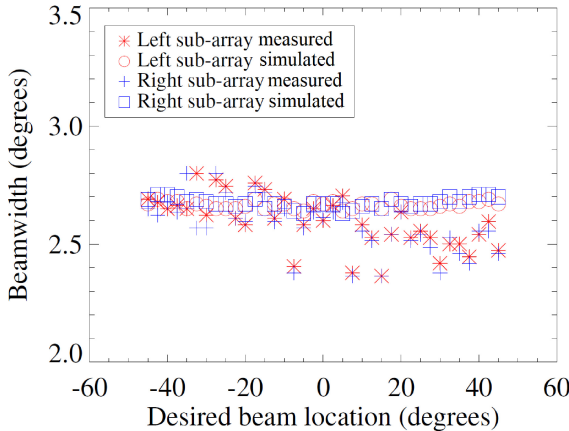


Fig. 3. Estimates of beamwidth from antenna-pattern measurements compared with corresponding simulation predictions for the implemented subarrays. In spite of neglecting mutual coupling and edge effects, simulations and measurements agree to first order.

for the receive patterns and as a receiver to measure transmit patterns. The radar was slowly slewed mechanically about the horn antenna, while rapid electronic scans were performed. The electronic scan was implemented as a sequence of discrete beams with a dwell time of 10 ms each. A slow mechanical slew allowed recording the power received by each beam over an azimuth span of 180°. Two comments about the measurement methodology are in order. First, both the horn and the phased-array antenna system were located only several meters above ground level. This in turn left some locations vulnerable to multipath effects in the vertical plane and limited the fidelity of gain measurements. Second, antenna pattern measurements are conventionally made rotating the aperture about its expected phase-center. For the spaced-antenna subarrays, this was not the case and the entire array was rotated about its physical center. But given the SA baselines investigated in this article are short relative to antenna azimuth dimension, we neglect errors due to asymmetric phase centers.

Fig. 3 shows derived antenna beamwidths along with the respective expected values for the 2.6° arrays as a function of scan angle. Note that the spaced-antenna systems close to broadside agree best with simulations. One possible explanation for the difference in measurements and simulations away from broadside are mutual coupling effects that are neglected by the simple simulation methodology used herein. The measurements of beamwidth are also of finite precision themselves. The net result of all this is that it may be advantageous to use the full correlation analysis (FCA) algorithm for subsequent spaced-antenna retrievals in electronically scanned systems. This is because the FCA algorithm does not require precise knowledge of the antenna pattern to retrieve the baseline wind.

Fig. 4 shows far-field pattern measurements of two-way antenna patterns synthesized for spaced-antenna subarrays at broadside. Some differences between the left and right synthesized beams are noticeable. As a practical matter, it is difficult to distinguish between systematic and random errors on subarrays using one measurement of the phased-array

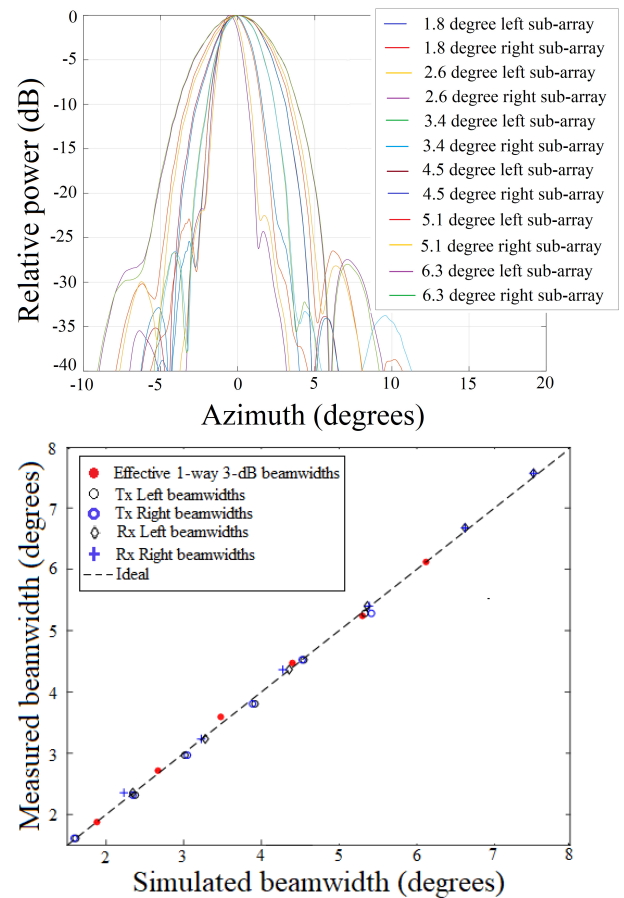


Fig. 4. (Top) Effective two-way antenna patterns of spaced-antenna systems with varying subarray sizes. The location of the beams and the shapes of the main beams only approximate desired patterns. (Bottom) Beamwidths of broadside patterns for various subarray implementations. At broadside, the subarray implementations are in much better agreement with simulations.

antenna system. For example, the residual errors in T/R module path phase compensation may have different statistics over short and long spatial scales. These errors may change over time. The net effect of all this is that it is more convenient to correct for beamforming errors in the retrieval process where possible, than to attempt to eliminate amplitude and phase errors completely. Notwithstanding, the left and right SA patterns appear matched to first order and the sidelobe levels are better than 20 dB. Furthermore, the bottom panel shows that beamwidths synthesized from the measurements agree well with simulations. Note that the simulations used herein neglect mutual coupling effects. As a consequence, the agreement between simulations and measurements is significantly better at broadside, as compared to higher scan angles.

B. Baseline Measurements

Spaced-antenna retrievals of baseline wind are based on a model for the correlation between received voltages [9]. A wide-sense stationary random process is assumed, and correlation function at short lags completely characterizes the random process. Herein, we exploit the same correlation function model to assess the baseline of the implemented

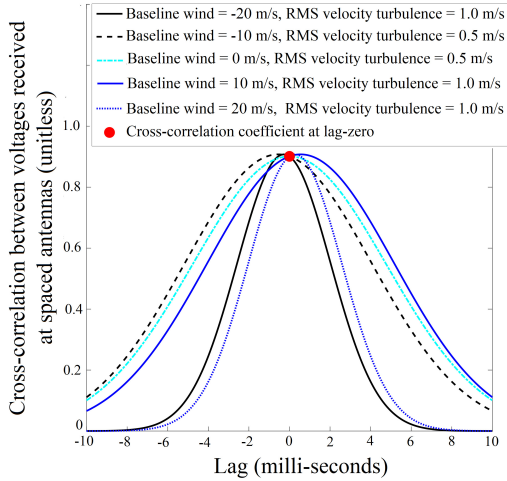


Fig. 5. Concept for SA baseline measurement. Note that the magnitude of the cross correlation γ is the same irrespective of wind speed. A one-way antenna beamwidth of 2.6° and a baseline of 8 cm were assumed.

spaced-antenna system. Fig. 5 shows that the cross correlation coefficient at zero-lag is invariant of wind field statistics. As the baseline wind and rms velocity turbulence change, we see that the cross correlation at zero-lag remains fixed while the peak and width of the correlation function change. Based on this property of a fixed cross correlation coefficient at lag-zero, an algorithm to derive baselines for spaced-antenna systems is as follows.

- 1) Measure beamwidth for each beam location using far-field methods. Denote each measurement of the equivalent beamwidth as $\hat{\phi}_e$ (in radians). This is related to the beamwidths of the left and right monostatic combinations by the relationship $\hat{\phi}_e^2 = (2/((1/(\sigma_{e\phi TR_L}^2)) + (1/(\sigma_{e\phi TR_R}^2))))$. Here, $\sigma_{e\phi TR_L}$ and $\sigma_{e\phi TR_R}$ are second central moments of the left and right spaced-antenna beams, respectively.
- 2) On precipitation echoes, estimate the cross correlation magnitude at lag-zero for each beam location. Denote each such measurement as $|\hat{\gamma}(\Delta x, 0)|$.
- 3) For each beam location, retrieve the baseline from the relationship [8]

$$\Delta \hat{x} = \sqrt{\frac{-\ln|\hat{\gamma}(\Delta x, 0)|16\ln(2)}{2k^2\hat{\phi}_e^2}}. \quad (1)$$

Here, k is the radar wavenumber. Other variables have been defined earlier.

Fig. 6 shows results that measure the relative phase-center displacement of the monostatic spaced-antenna combinations. For this figure, the simulations employ the measured beamwidths in Fig. 3. The cross correlation coefficient estimates were obtained using the spectral moments method described in [5] because it allowed for simple filtering of ground clutter. The following quality control metrics were used to selectively average the cross correlation coefficient for a given beam location.

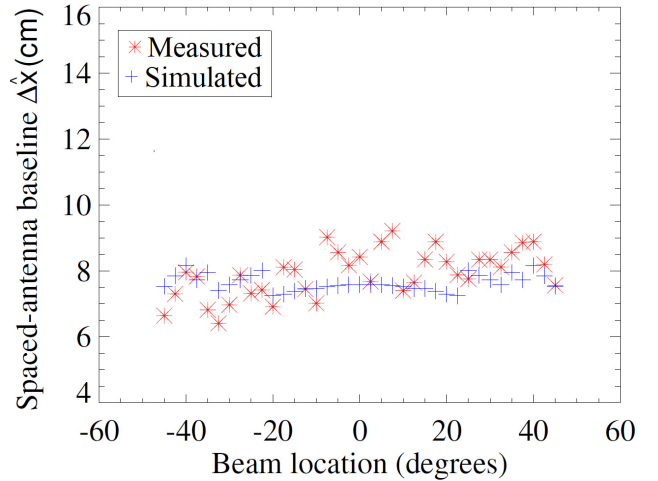


Fig. 6. Synthesized spaced-antenna baselines for the 2.6° equivalent one-way beamwidth design. The good agreement between simulated baselines and measured baselines validates the implementation of this design.

- 1) Spectrum with greater than 1 m/s. Since the baseline measurement algorithm employed requires volume scattering, this threshold removes ground clutter artifacts.
- 2) SNR greater than 20 dB. This threshold effectively removes effects of noise “spikes” of the cross correlation at zero-lag because of elements common to both apertures.

The agreement of the measured baselines with expected values effectively validates the algorithm for baseline measurement. Note that the good performance of the algorithm was a direct result of the high cross correlation coefficient at lag-zero. Had wider beams or longer baselines been employed, the fidelity of the baselines measured with this algorithm would have degraded.

C. Beam Squint Measurements

Active phased-array spaced-antenna systems have two kinds of beam pointing errors. The first type is a relative beam pointing error that occurs between the transmit and receive antenna patterns. This type of beam pointing error does not directly affect the fidelity of the spaced-antenna retrievals but degrades the system SNR. The second type is a relative squint between the left and right spaced-antenna systems. This latter type of beam squint has a direct effect on the spaced-antenna retrievals and is the primary focus herein. Fig. 7 shows a comparison in beam squinting errors for the implemented broadside spaced-antenna systems. We note that short baselines have little differential squint between the left and right spaced-antenna systems. This is because of element level errors are retained on spaced-antenna systems with significant overlap. But the differential beam squint errors show a systematic increase as a function of baseline. This is because systematic errors such as incorrect interelement spacing knowledge become more pronounced as the baseline increases and contribute more significantly to differential beam squint between the left and right SA systems.

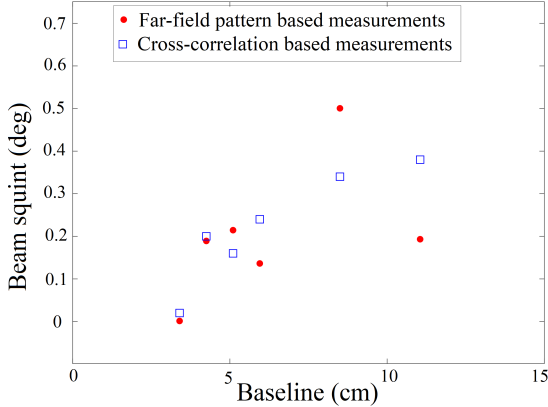


Fig. 7. Difference between beam pointing angles of the left and right SA systems. Both far-field pattern measurements and the cross correlation based method show that SA systems with short baselines and largest number of overlapping elements have the least beam squint.

For the X-band active phased-array system used herein, beam squint errors in the synthesized spaced-antenna were directly proportional to the baseline. However, it is worth noting that the implemented SA systems used to arrive at Fig. 7 had smaller apertures as the baselines were increased. This had the effect of creating exaggerated slopes in Fig. 7—which allow for clear argument that high overlap in apertures minimizes beam squint errors. On the other end, we did not consider baselines shorter than 3 cm because the corresponding spaced-antenna retrievals have poor immunity to thermal noise.

IV. CONCLUSION

To date, literature on adapting the SA concept to microwave weather radars has been largely focused on theoretical modeling and simulation-based studies. The lack of success in spaced-antenna weather radar implementations to date may, in part, be attributed to difficulty in optimizing system design. In this article, we investigated aperture synthesis for an X-band SA weather radar using a flexible active phased-array concept. Segmenting an active array face into subarrays with displaced phase-centers, a variety of spaced-antenna weather radar implementations were examined. Far-field antenna patterns of these spaced-antenna systems were measured by stepping through the beams to be evaluated while slowly mechanically scanning the antenna array face past a beacon.

The figures of merit used to evaluate spaced-antenna aperture synthesis were beamwidth errors, baseline errors and relative squint between the left/right spaced-antenna systems. In examining beamwidth and beam squint errors relative to

simulated expectations, antenna far-field pattern measurements were of primary importance. The reasonable agreement of simulated results with measurements validated the simulation methodology employed herein. Using these simulated expectations as a prognostic, real data collected with the X-band phased-array was used to demonstrate a novel method to measure the spaced-antenna baseline based on received echo statistics. This algorithm exploited the invariance of the cross correlation function at lag-zero to meteorological parameters such as wind speed and rms velocity turbulence. By taking advantage of prior knowledge of radar wavenumber and beamwidth, this technique allows for “in-place” calibration of SA systems and can be used to compensate for inevitable T/R module failures as they occur. Existing SA profilers such as the multiple antenna profiler (MAPR) [2] and the Jicamarca radio observatory [10] may readily incorporate this method. Finally, we find that highly overlapping spaced-antenna arrays were most immune to relative beam squint errors between the left and right SA systems. This is because element level errors are retained on the left and right SA systems, thereby minimizing the impact on differential beam squint.

REFERENCES

- [1] B. H. Briggs, G. J. Phillips, and D. H. Shinn, “The analysis of observations on spaced receivers of the fading of radio signals,” *Proc. Phys. Soc. London, B*, vol. 63, no. 2, pp. 106–121, Feb. 1950.
- [2] S. A. Cohn, W. O. J. Brown, C. L. Martin, M. E. Susedik, G. D. Maclean, and D. B. Parsons, “Clear air boundary layer spaced antenna wind measurement with the multiple antenna profiler (MAPR),” *Annales Geophysicae*, vol. 19, no. 8, pp. 845–854, 2001.
- [3] A. Pazmany, H. B. Bluestein, M. M. French, and S. Frasier, “Observations of the two-dimensional wind field in severe convective storms using a mobile, X-band, Doppler radar with spaced antenna,” in *Proc. 22nd Conf. Severe Local Storms*. Hyannis, MA, USA: AMS, 2004, p. P7.3.
- [4] G. Zhang and R. J. Doviak, “Spaced-antenna interferometry to measure crossbeam wind, shear, and turbulence: Theory and formulation,” *J. Atmos. Ocean. Technol.*, vol. 24, no. 5, pp. 791–805, May 2007.
- [5] V. Venkatesh and S. J. Frasier, “Simulation of spaced antenna wind retrieval performance on an X-band active phased array weather radar,” *J. Atmos. Ocean. Technol.*, vol. 30, no. 7, pp. 1447–1459, Jul. 2013.
- [6] K. A. Orzel and S. J. Frasier, “Weather observation by an electronically scanned dual-polarization phase-tilt radar,” *IEEE Trans. Geosci. Remote Sens.*, vol. 56, no. 5, pp. 2722–2734, May 2018.
- [7] J. L. Salazar, E. J. Knapp, and D. J. McLaughlin, “Dual-polarization performance of the phase-tilt antenna array in a casa dense network radar,” in *Proc. IEEE Int. Geosci. Remote Sens. Symp.* Honolulu, HI, USA: IEEE, Jul. 2010, pp. 3470–3473.
- [8] V. Venkatesh, “Spaced-antenna wind estimation using an X-band active phased array weather radar,” Ph.D. dissertation, Dept. Elect. Comput. Eng., Univ. Massachusetts Amherst, Amherst, MA, USA, 2013.
- [9] R. J. Doviak, R. J. Lataitis, and C. L. Holloway, “Cross correlations and cross spectra for spaced antenna wind profilers: I. Theoretical analysis,” *Radio Sci.*, vol. 31, no. 1, pp. 157–180, Jan. 1996.
- [10] J. L. Chau, R. J. Doviak, A. Muschinski, and C. L. Holloway, “Tropospheric measurements of turbulence and characteristics of Bragg scatterers using the Jicamarca VHF radar,” *Radio Sci.*, vol. 35, no. 1, pp. 179–193, Jan. 2000.